



HAL
open science

Foot adaptation to climbing in ovenbirds and woodcreepers (Furnariida)

Killian Leblanc, Romain Pintore, Ana Galvão, Ezekiel Heitz, Pauline Provini

► **To cite this version:**

Killian Leblanc, Romain Pintore, Ana Galvão, Ezekiel Heitz, Pauline Provini. Foot adaptation to climbing in ovenbirds and woodcreepers (Furnariida). *Journal of Anatomy*, In press, 10.1111/joa.13805 . hal-03971743

HAL Id: hal-03971743

<https://hal.science/hal-03971743>

Submitted on 16 Mar 2023

HAL is a multi-disciplinary open access archive for the deposit and dissemination of scientific research documents, whether they are published or not. The documents may come from teaching and research institutions in France or abroad, or from public or private research centers.



L'archive ouverte pluridisciplinaire **HAL**, est destinée au dépôt et à la diffusion de documents scientifiques de niveau recherche, publiés ou non, émanant des établissements d'enseignement et de recherche français ou étrangers, des laboratoires publics ou privés.



Distributed under a Creative Commons Attribution - NonCommercial - NoDerivatives 4.0 International License

ORIGINAL ARTICLE

Foot adaptation to climbing in ovenbirds and woodcreepers (Furnariida)

Killian Leblanc^{1,2} | Romain Pintore^{3,4}  | Ana Galvão⁵  | Ezekiel Heitz^{1,2,3} | Pauline Provini^{1,2,3} 

¹Université Paris Cité, Inserm, System Engineering and Evolution Dynamics, Paris, France

²Learning Planet Institute, Paris, France

³UMR 7179 C.N.R.S/M.N.H.N. MECADEV, Département Adaptations du Vivant, Paris, France

⁴Structure and Motion Laboratory, Department of Comparative Biomedical Sciences, Royal Veterinary College, Hatfield, UK

⁵Laboratório de Ornitologia, Departamento de Zoologia, Universidade Federal do Rio de Janeiro, Rio de Janeiro, Brazil

Correspondence

Pauline Provini, Bâtiment d'Anatomie Comparée CP55, 55 rue Buffon, 75005 Paris, France.

Email: pauline.provini@mnhn.fr

Funding information

CRI Research Fellowship; Fondation Bettencourt Schueller; Programa Nacional de Pós-Doutorado (PNPD) of the Coordenação de Aperfeiçoamento Pessoal de Nível Superior (CAPES, Brazil); European Research Council; TEMPO, Grant/Award Number: ERC-2015-STG-677774; oVert TCM; Duke University; Macaulay Library at the Cornell Lab of Ornithology, Grant/Award Number: ML33078331 and ML66570301

Abstract

Furnariida (i.e. ovenbirds, woodcreepers and antbirds) cover diverse ecologies and locomotor habits, ranging from strictly terrestrial to climbing birds, with different degrees of acrobatic performances. We know that this variety of locomotor modes is linked to different limb morpho-functional adaptations in other climbing clades of birds, such as woodpeckers and nuthatches. Here, we link the morphological variations to ecological categories, such as different locomotor habits and a gradient of acrobatic performances, in a phylogenetically informed analysis. We used a high-density three-dimensional (3D) geometric morphometric approach on foot bones (tarsometatarsus and all toes) of 55 specimens from 39 species of Furnariida. We found a significant correlation between acrobatic performances and foot bone shapes, partly explained by the phylogenetic relationship between species. Dendrocolaptidae show specific anatomical features, linked to their acrobatic locomotor habits. More specifically, we found that: (1) foot bones are more robust amongst climbing Furnariida, (2) the spread between toes is wider amongst highly acrobatic Furnariida, (3) dermal syndactyly between digits II and III is linked to special osteological features interpreted as functional osteological syndactyly in woodcreepers (tail-assisted climbers) and (4) the hallux claw is straighter than other claws in climbing Furnariida. Our study demonstrates that climbing Furnariida evolved common foot adaptations with subtle phenotypic variations depending on their climbing performances, refining our understanding of how evolution shapes interactions amongst structure, function and ecological traits.

KEYWORDS

arboreal, claw, Passeriformes, scansorial, syndactyly, tarsometatarsus

Killian Leblanc and Romain Pintore are co first authors.

This is an open access article under the terms of the [Creative Commons Attribution-NonCommercial](https://creativecommons.org/licenses/by-nc/4.0/) License, which permits use, distribution and reproduction in any medium, provided the original work is properly cited and is not used for commercial purposes.

© 2022 The Authors. *Journal of Anatomy* published by John Wiley & Sons Ltd on behalf of Anatomical Society.

1 | INTRODUCTION

Climbing species are rare across birds, probably because it is a challenging type of locomotion amongst animals with forelimbs adapted to flight (Cartmill, 1985). Climbing are mainly found in three groups of birds so far: Picidae (e.g. woodpecker counting 240 species), Certhioidea (e.g. nuthatch, treecreeper, and wallcreeper with 154 species), and Furnariida (e.g. Furnariidae or ovenbirds counting 240 species and Dendrocolaptidae or woodcreepers 57 species). Most climbing birds, including Certhioidea and Furnariida have anisodactyl feet (i.e. hallux oriented backwards whilst digits II, III, and IV are oriented forward). This foot configuration should be more favourable for climbing as the three digits oriented forward provide more strength to pull out the body when climbing (Bock & Miller, 1959). In contrast, woodpeckers have zygodactyl feet (hallux and digit IV are oriented backwards whilst digits II and III are oriented forward). Yet, in some woodpeckers like *Dendrocopos villosus*, digit IV can rotate to the side giving a configuration similar to anisodactyl birds, the hallux can even be lost in species such as *Picoides tridactylus* (Bock & Miller, 1959). These observations suggest that constraints associated with climbing can lead to potentially convergent morphological features. Previous work explored foot shape in birds, at the osteological (Abourachid et al., 2017; Provini & Höfling, 2020) and skin levels (Höfling & Abourachid, 2021) on a large sample of bird species, of different toe configurations and degree of arboreality. They found that osteological features are linked to the toe orientation and the degree of terrestriality (Abourachid et al., 2017), for example, that phalanges tend to be enlarged in climbing birds, especially for the proximal hallux phalanx (Abourachid et al., 2017). In addition, they observed that syndactyly, the toe fusion at different degrees, is common in perching birds (Höfling & Abourachid, 2021). Here, we propose to investigate the relationship between foot shape and locomotor habits, by focusing on a group of acrobatic anisodactyl birds, the Furnariida.

Although woodpeckers received most of the attention (Bock, 1999; Bock & Miller, 1959; Scharnke, 1930; Spring, 1965), the diversity of locomotor behaviours amongst Furnariida is also worthwhile. This clade is endemic to the Neotropics and reckons 663 species distributed in 10 families (Moyle et al., 2009; Ohlson et al., 2013). Species from the *Phylidor* genus and the well-named *Acrobatornis* genus can perform acrobatic poses (Pacheco et al., 1996; Parrini et al., 2010), whereas others are strictly terrestrial like *Furnarius rufus*, displaying hopping or walking habits (Fraga, 1980; Krabbe & Schulenberg, 2003; Sick et al., 1997). Dendrocolaptidae and Furnariidae are sister groups (Irestedt et al., 2002; Moyle et al., 2009; Ohlson et al., 2013). Whilst all Dendrocolaptidae species are good vertical climbers, Furnariidae, on the contrary, present a much greater diversity of locomotion types, ranging from terrestrial to highly acrobatic and arboreal habits (Irestedt et al., 2002; Moyle et al., 2009; Ohlson et al., 2013). Dendrocolaptidae are all tail-assisted climbers, using their tail feathers, with thick and curved rachis, to support the body when climbing, whereas Furnariidae only rely on their hindlimbs. These contrasting climbing strategies within these two Furnariida families suggest

potential dissimilarities in the morphological adaptation of their locomotor apparatus. Indeed, whilst tail-assisted climbers tend to have shortened toes (Bock & Miller, 1959; Feduccia, 1973), birds like nuthatches (Sittidae) have elongated toes thought to increase their grasp on trunks (Cartmill, 1985).

To our knowledge, no 3D quantitative analysis of the entire foot morphology, including all autopod bones, has been performed on climbing Furnariidae, leaving open the possibility of shared morphological features amongst Furnariida that might be connected to their climbing adaptations. To explore this, we studied the entire foot, including all of the 14 phalanges, which are directly in contact with the substrate during terrestrial locomotion, as well as the tarsometatarsus, which connects the phalanges with the rest of the body. We assumed that the shape of the terminal phalanx (i.e. ungual bone) reflects the shape of the keratin sheath (Hedrick et al., 2019). Previous works observed that the foot of climbing Furnariida presents a fusion of the proximal basal phalanges for digits II–III and IV (Feduccia, 1973). This fusion was only observed at a dermal level but seems to occur regularly within birds showing greater performance at climbing or clinging along tree trunks. In perching birds, syndactyly is relatively common and primarily affects proximal phalanges (Höfling & Abourachid, 2021). Even if we analysed the entire bone dataset we focus our discussion on the tarsometatarsus, the first phalanges of each finger and the hallux ungual bone.

Computed tomography (CT) scanning methods provided highly accurate 3D models of foot bones, some of them being very small (4 mm for the first phalanx of the hallux of *Glyphorhynchus spirurus*). This allowed us to study morphological traits with climbing adaptations, using a 3D geometric morphometric (3D GMM) approach, combining anatomical and sliding semilandmarks on a large sample of Furnariida foot bones. We then investigated how their morphologies varied between groups of different locomotor habits and perching performances. The goal of this study was to identify shared morphological traits, amongst Furnariida, that may be related to their climbing adaptations, in a phylogenetically informed context.

2 | MATERIALS AND METHODS

2.1 | Bird sample

We collected the tarsometatarsus bone and all phalanges, from 39 species across all families of Furnariida (Table 1). Amongst them, 15 species were represented by two specimens, which makes 55 specimens. We observed the presence and absence of syndactyly at a dermal level for each specimen (Table 1).

A total of 48 specimens, from 39 different species, came from the Coleção Ornitológica do Instituto de Biologia of the Universidade Federal do Rio de Janeiro and the Coleção Ornitológica of the Museu Paraense Emílio Goeldi, Brazil. The specimens showed no signs of abnormality and had all foot bones intact, with fused epiphyses. The specimens were scanned at the micro-CT scan imaging facility of the Instituto de Biociências of

TABLE 1 Summary of the specimens used in the study, with the classification of the locomotor groups, perching performance groups, as well as the bones involved in the osteological syndactyly when present

Taxonomy	Abb.	Locomotor group	Perching performance	Syndactyly	Source	ID
Conopophagidae						
<i>Conopophaga melanops</i>	mel	Hop	Low	DII-DIII DIII-DIV	UFRJ	UFRJ919
Dendrocolaptidae						
<i>Sittasomus griseicapillus</i>	gri	Climb	High	NA	UFRJ	UFRJ1769
<i>Dendrocincla turdina</i>	tur	Climb	High	DII-DIII DIII-DIV	UFRJ	UFRJ922
<i>Campylorhamphus falcularius</i>	fal	Climb	High	DII-DIII DIII-DIV	UFRJ	UFRJ1932
<i>Campylorhamphus falcularius</i>	fal	Climb	High	DII-DIII DIII-DIV	UFRJ	UFRJ1947
<i>Sittasomus griseicapillus</i>	gri	Climb	High	DII-DIII DIII-DIV	UFRJ	UFRJ2009
<i>Xiphocolaptes albicollis</i>	alb	Climb	High	DII-DIII DIII-DIV	UFRJ	UFRJ2016
<i>Xiphocolaptes albicollis</i>	alb	Climb	High	DII-DIII DIII-DIV	UFRJ	UFRJ2017
<i>Glyphorhynchus spirurus</i>	spr	Climb	High	DII-DIII DIII-DIV	UFRJ	UFRJ1951
<i>Hylexetastes perrotii</i>	per	Climb	High	DII-DIII DIII-DIV	UFRJ	UFRJ1958
<i>Deconychura longicauda</i>	lon	Climb	High	DII-DIII DIII-DIV	UFRJ	UFRJ1961
<i>Glyphorhynchus spirurus</i>	spr	Climb	High	DII-DIII DIII-DIV	UFRJ	UFRJ1968
Formicariidae						
<i>Chamaeza ruficauda</i>	rfi	Walk	Low	DIII-DIV	UFRJ	UFRJ1125
<i>Chamaeza ruficauda</i>	rfi	Walk	Low	DIII-DIV	UFRJ	UFRJ1946
<i>Formicarius colma</i>	col	Walk	Low	DIII-DIV	UFRJ	UFR920
Furnariidae						
<i>Anabazenops fuscus</i>	fus	Hop	High	DII-DIII DIII-DIV	UFRJ	UFRJ2015
<i>Aphrastura spinicauda</i>	spi	Climb	High	NA	Morphosource	FMNH:birds:314046
<i>Automolus leucophthalmus</i>	leu	Hop	Medium	DII-DIII DIII-DIV	UFRJ	UFRJ1937
<i>Furnarius rufus</i>	ruf	Walk	Low	DIII-DIV	Morphosource	FMNH:birds:105658
<i>Furnarius rufus</i>	ruf	Walk	Low	DIII-DIV	UFRJ	UFRJ1934
<i>Gyalophylax hellmayri</i>	hel	Hop	Low	NA	UFRJ	ANA18
<i>Lochmias nematura</i>	nem	Hop	Medium	DIII-DIV	UFRJ	UFRJ2011
<i>Lochmias nematura</i>	nem	Hop	Medium	DIII-DIV	UFRJ	UFRJ2012
<i>Phacellodomus rufifrons</i>	rff	Hop	Low	DII-DIII DIII-DIV	UFRJ	UFRJ2033
<i>Phacellodomus rufifrons</i>	rff	Hop	Low	DII-DIII DIII-DIV	UFRJ	RBO1013
<i>Philydor atricapillus</i>	atr	Hop	High	DII-DIII DIII-DIV	UFRJ	UFRJ1161
<i>Philydor atricapillus</i>	atr	Hop	High	DII-DIII DIII-DIV	UFRJ	UFRJ1940
<i>Roraimia adusta</i>	adu	Climb	High	NA	Morphosource	FMNH:birds:335140
<i>Sylviorthorhynchus desmursii</i>	des	Hop	High	NA	Morphosource	FMNHB:birds:343607
<i>Xenops minutus</i>	min	Climb	High	DII-DIII DIII-DIV	UFRJ	UFRJ1936
<i>Xenops minutus</i>	min	Climb	High	DII-DIII DIII-DIV	UFRJ	UFRJ2019
Grallariidae						
<i>Hylopezus paraensis</i>	par	Hop	Low	DIII-DIV	UFRJ	UFRJ1935
Melanopareiidae						
<i>Melanopareia bitorquata</i>	bit	Hop	Low	NA	Morphosource	FMNH:birds:335140
Rhinocryptidae						
<i>Merulaxis ater</i>	ate	Walk	Low	DIII-DIV	UFRJ	UFRJ0862
Scleruridae						
<i>Sclerurus scansor</i>	sca	Hop	Low	DII-DIII DIII-DIV	UFRJ	UFRJ2008
<i>Sclerurus scansor</i>	sca	Hop	Low	DII-DIII DIII-DIV	UFRJ	UFRJ2018

(Continues)

TABLE 1 (Continued)

Taxonomy	Abb.	Locomotor group	Perching performance	Syndactyly	Source	ID
Thamnophilidae						
<i>Myrmorchilus strigilatus</i>	str	Walk	Low	NA	UFRJ	ANA26
<i>Euchrepomis spodioptila</i>	spo	Hop	Medium	NA	Morphosource	FMNH:birds:344009
<i>Hypocnemoides maculicauda</i>	mac	Hop	Low	DII-DIII DIII-DIV	UFRJ	UFRJ1328
<i>Willisornis poecilinotus</i>	poe	Hop	Medium	DII-DIII DIII-DIV	UFRJ	UFRJ1964
<i>Myrmoderus loricatus</i>	lor	Hop	Low	DIII-DIV	UFRJ	UFRJ855
<i>Hypoedaleus guttatus</i>	gut	Hop	Medium	DIII-DIV	UFRJ	UFRJ1935
<i>Dysithamnus mentalis</i>	men	Hop	Medium	DIII-DIV	UFRJ	UFRJ1944
<i>Thamnophilus caeruleus</i>	cae	Hop	Medium	DIII-DIV	UFRJ	UFRJ1945
<i>Hypoedaleus guttatus</i>	gut	Hop	Medium	DIII-DIV	UFRJ	UFRJ2013
<i>Mackenziaena severa</i>	sev	Hop	Medium	DIII-DIV	UFRJ	UFRJ2014
<i>Phlegopsis nigromaculata</i>	nig	Hop	Medium	DII-DIII DIII-DIV	UFRJ	UFRJ1971
<i>Willisornis poecilinotus</i>	poe	Hop	Medium	DII-DIII DIII-DIV	UFRJ	UFRJ1980
<i>Dysithamnus mentalis</i>	men	Hop	Medium	DIII-DIV	UFRJ	UFRJ744
<i>Dryophila squamata</i>	squ	Hop	Medium	DIII-DIV	UFRJ	UFRJ475
<i>Dryophila squamata</i>	squ	Hop	Medium	DIII-DIV	UFRJ	UFRJ480
<i>Dryophila squamata</i>	squ	Hop	Medium	DIII-DIV	UFRJ	UFRJ481
<i>Myrmotherula axillaris</i>	axi	Hop	Medium	DIII-DIV	UFRJ	UFRJ932
<i>Sakesphorus cristatus</i>	cris	Hop	Low	DIII-DIV	UFRJ	UFRJ938
<i>Myrmornis torquata</i>	tor	Hop	Low	NA	Morphosource	YPM:birds:106157

the Universidade de São Paulo Brazil with a SkyScan 1176 microtomographer (BrukerMicroCT, 2003). The resolution was adjusted depending on the size of the specimens from 9 μm (45 kV, 300 μA) to 18 μm (80 kV, 250 μA).

We added seven specimens from MorphoSource (www.morphosource.org) (SM1). For *Myrmornis torquata*, only the proximal phalanges and the unguis bone of the three first unguis bones were available. We excluded *Phacellodomus rufifrons* and *Furnarius rufus* for the unguis bone of digit II analysis because they were too damaged. The phalanx IV of the digit III was missing for the *Phacellodomus rufifrons* and *Campylorhamphus falcularius* (UFRJ1947). *Campylorhamphus falcularius* also missed phalanges III of digit III and phalanx IV of digit IV. We excluded both specimens of *Xenops minutus* as the phalanx III of digit IV was poorly preserved.

2.2 | 3D modelling

We segmented the CT scans using Avizo (v. 9.7, FEI Visualisation Sciences Group). For each specimen, we only retained the right side; when the right side was not available, we segmented the left side and mirrored it, using the function "mirror" in the Blender software (v. 3.0, Blender Online Community, 2014). The 3D models were imported in Geomagic Wrap (v. 2013.001, 3D Systems, 2013). We used the function "remesh", and "clean" to remove and clean artefacts manually, making sure the initial shape of the specimen was preserved.

2.3 | 3D geometric morphometrics

Bone shape variation was quantified using 3D GMM. We digitised anatomical landmarks on every bone and added sliding semilandmarks on curves and surfaces for the phalanges. We chose not to use semilandmarks on the tarsometatarsus because ossified tendons on the ventral side (Raikow, 1994) could interfere with the interpretation of its shape. We followed the protocol previously recommended (Botton-Divet et al., 2015; Gunz et al., 2005; Gunz & Mitteroecker, 2013) to digitise the anatomical landmarks and semilandmark on curves and surfaces, using the IDAV Landmark software (v. 3.0.0.6, Wiley et al., 2005).

We used 36 anatomical landmarks for the tarsometatarsus, nine for the unguis phalanx and five for the other phalanges. We added 36 sliding semilandmarks on curves for each unguis phalanx and 16 for the rest of the phalanges. We manually placed all sliding surface semilandmarks varying in a range between 119 to 553 for unguis phalanges and 164 to 574 for the other phalanges (Figure 1, SM2). For bones with sliding semilandmarks (i.e. phalanges), we digitised each anatomical landmark and sliding semilandmarks along curves. Then, we manually digitised sliding semilandmarks along the surfaces of one specimen per bone (*Hylopezus macularius*, A8409), considered as "the template" (Cornette et al., 2013). To obtain homologous landmark coordinates between all specimens, we used the R package Morpho (v. 2.9; Schlager, 2017) to perform several spline relaxations that minimized the bending energy of a Thin Plate Spline (TPS). First, we used the "placePatch" function to automatically

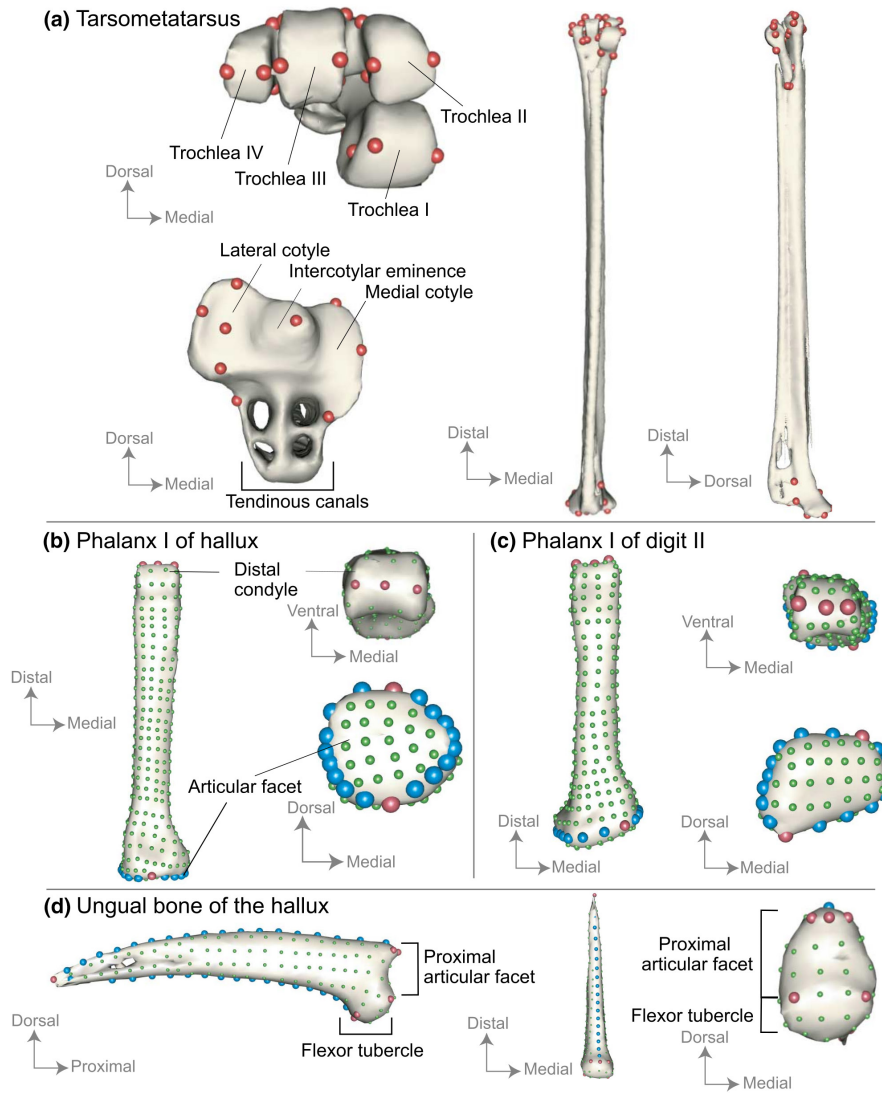


FIGURE 1 Landmarks template. Templates of *Hylopezus paraensis*. (a) the tarsometatarsus; (b) the first phalanx of the hallux; (c) the first phalanx of the digit II and (d) the ungual bone of the hallux. Red spheres correspond to anatomical landmarks, green spheres correspond to manual semilandmarks and blue spheres correspond to automatic curves

project the surface semilandmarks of the template onto every other specimen, following the interpolation of sliding semilandmarks along curves. Then, we performed five iterations of another spline relaxation between landmark configurations of the template and the other specimens with the function “relaxLM”. Finally, we conducted two iterations of a final spline relaxation between a mean landmark configuration and the one from all specimens using the “slideLM” function. These steps ensured that all landmark configurations within each bone dataset were geometrically homologous and that shifts in the coordinates of corresponding landmarks could be interpreted as morphological variations (Gunz et al., 2005). We conducted a Generalised Procrustes Analysis (GPA) with the “procSym” function to superimpose the landmark configurations and make them spatially homologous in the Cartesian coordinate system (Rohlf, 1990). We performed a Principal Component Analysis (PCA) to describe shape variation using “prcomp” from the R package stats (v. 4.1.2; R Core Team et al., 2018).

We performed a repeatability test to quantify the operator's ability to reproduce the same landmark configuration across several specimens. To do so, we selected three morphologically close specimens found on preliminary PCA for each bone and digitised 10 times the same landmark configuration (single anatomical landmarks only) for each specimen. We visualised the result with PCA and looked for overlap between species. We found no overlap for each bone, which indicates that there is no bias (SM3).

2.4 | Locomotor groups

From literature and video recordings (SM4), we classified the 55 studied species into three locomotor categories: “walk”, “hop” and “climb”, corresponding to their most used way of locomotion (Provini & Höfling, 2020). As some hopping birds predominantly hop on the ground, they face a different physical stress compared

to birds hopping on trees (Zeffert et al., 2003). Therefore, we created three additional performance categories, reflecting birds' abilities to achieve acrobatic and complex manoeuvres. High-performance group includes birds able to climb on trees and/or to use complex perching manoeuvres, such as hang-upside down and hang-down on a regular basis (Figure 2). The medium-performance group includes perching birds, able to hang sideways and occasionally use relatively complex manoeuvres, such as hang-down and hang-upside down, but less often than birds in the high-performance group. The low-performance group includes birds that mostly hop or walk on the ground, but rarely use complex perching manoeuvres, and prefer perching on horizontal or inclined perch.

2.5 | Phylogeny and multivariate statistical analysis

We constructed a phylogenetic tree based (SM5) on the most recent phylogeny including all species present in our sample (Moyle et al., 2009) using the software Mesquite (v. 3.61; Maddison and Maddison, 2007) and set the branch length to one.

We used R (v. 4.1.2, (Team, 2021)) to perform our statistical tests and visualisations. We plotted the PCA for each bone as well as the shape deformation associated with each PCA axis (Figures 3–8, SM6, SM7). We checked if there was a significant effect of size on the shape (i.e. evolutionary allometry) and quantified this relationship (Klingenberg, 2016). We used the PC scores, log-transformed centroid sizes, and the reconstructed phylogeny as the main arguments. We performed a phylogenetic generalised least square (PGLS) test with the “procD.pgls” function of the R package geomorph (v4.0.3; Adams et al., 2022) between (1) all the PC scores and (2) the two first PC axes individually with the log-transformed centroid size to investigate allometric effects across the dataset, representing each isolated morphological variation (SM8a and b).

We plotted the phylomorphospace associated with the PCA, using the “gm.prcmp” function of the Geomorph package (Figures 3–8 and SM6). We also tested the phylogenetic signals using the “physignal” function of the package geomorph with our reconstructed tree at a multidimensional level (i.e. considering all the PCs) and at a unidimensional level on the isolated two first PCs (SM8B). The K_{mult} test, derived from the K statistics (Blomberg et al., 2003),

(a) *Anabacerthia lichtensteini*



(b) *Anabacerthia variegaticeps*



(c) *Philydor atricapillus*



FIGURE 2 Acrobatic stances illustration. Photos illustrating the acrobatic poses of three species of Furnariida: (a) hanging head down on a subvertical perch (*Anabacerthia lichtensteini*); (b) hanging upside-down on a subhorizontal perch (*Anabacerthia variegaticeps*); (c) hanging upside-down (*Philydor atricapillus*). Full credit to the contributors of eBird for the photos (SM4a)

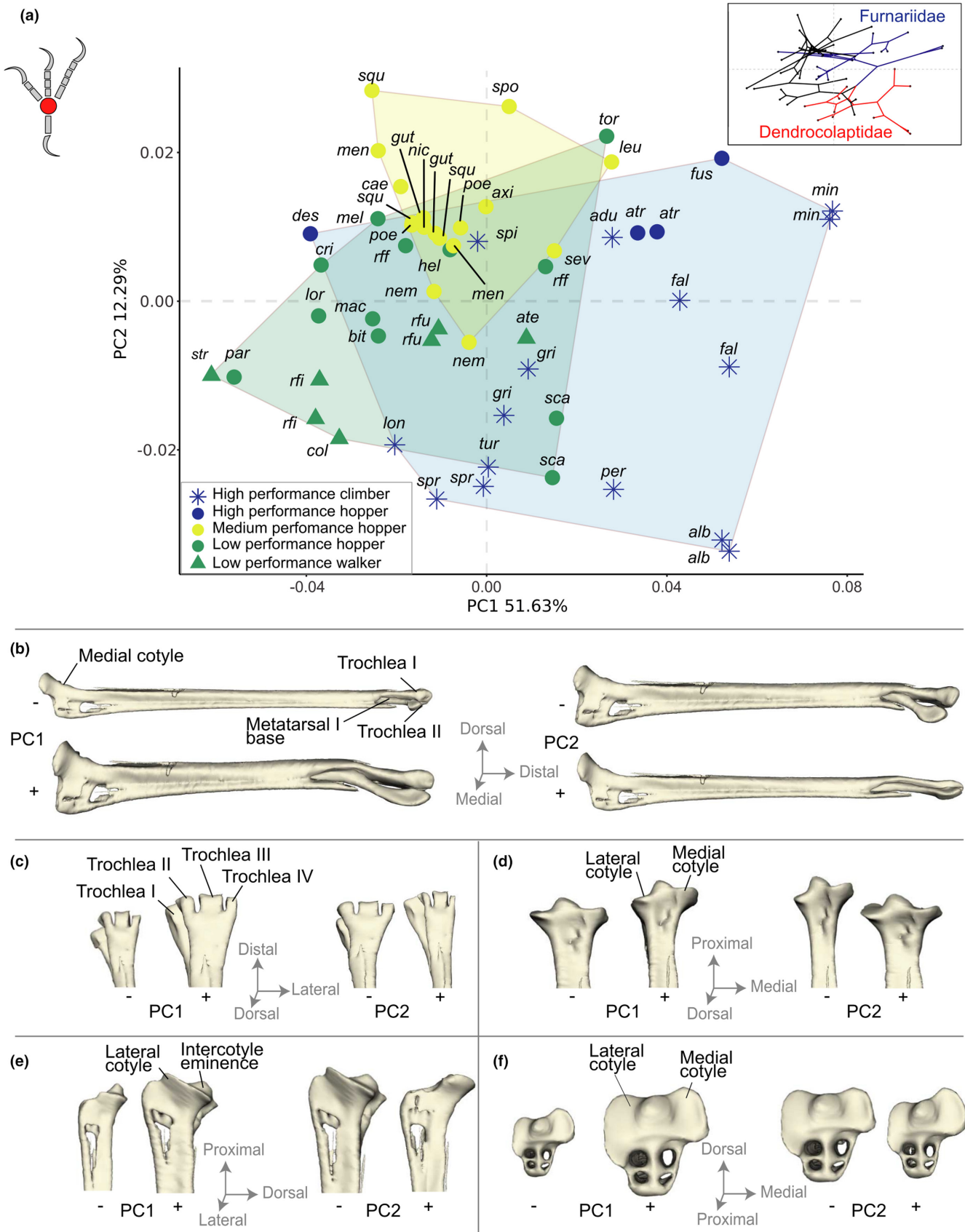


FIGURE 3 Geometric morphometric results for the tarsometatarsus. (a) PCA morphospace for the tarsometatarsus, a phylomorphospace is presented with the two main phylogenetic groups coloured (Furnariidae in blue, Dendrocolaptidae in red). Shape deformation at both extrema along PC1 (left) and PC2 (right) in (b–f). TPS deformations are mapped on *Hylopezus macularius* (A8409)

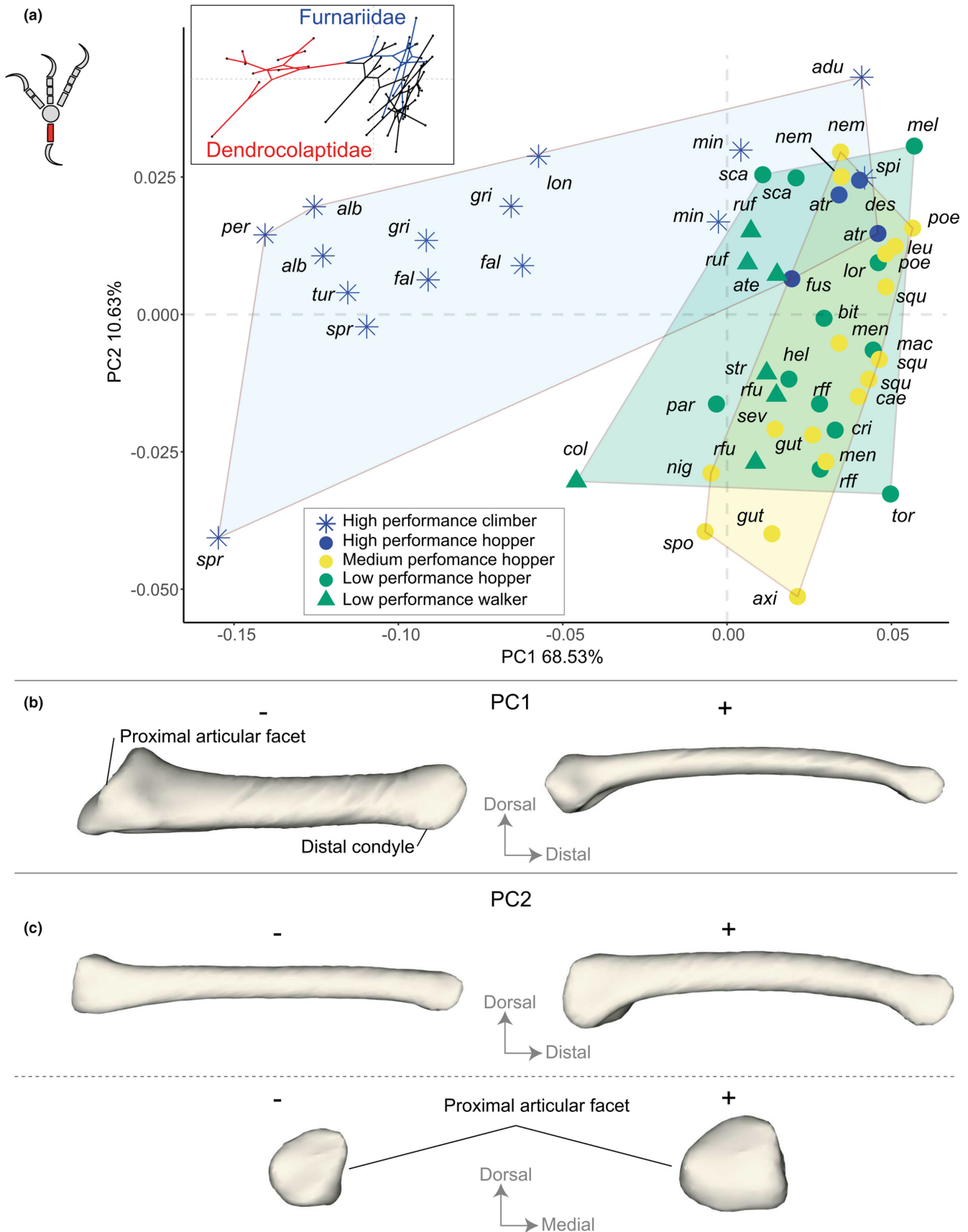
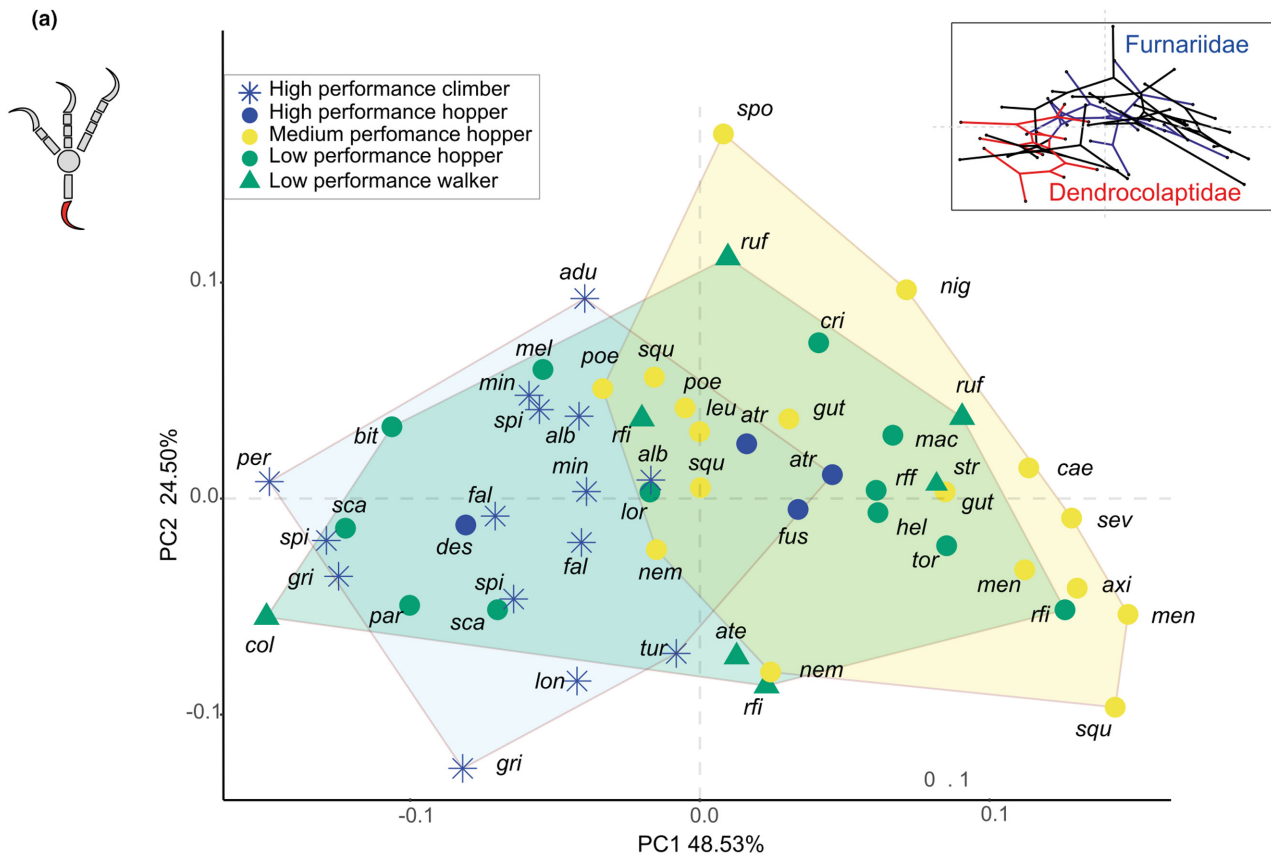
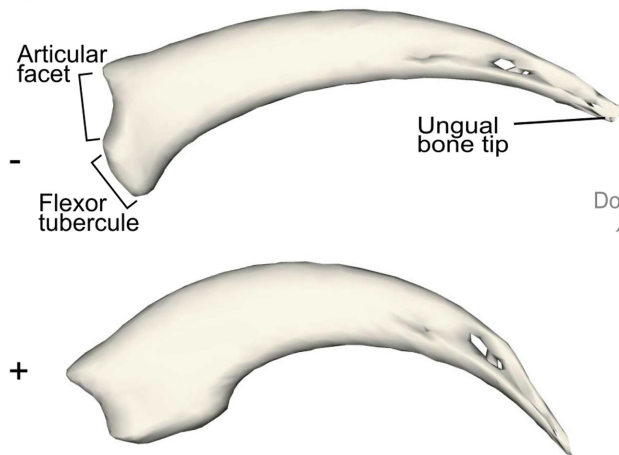


FIGURE 4 Geometric morphometric results for the first phalanx of the hallux. (a) PCA morphospace for the first phalanx of the hallux, a phylomorphospace is presented with the two main phylogenetic groups coloured (Furnariidae in blue, Dendrocolaptidae in red). Shape deformation at both Extrema along PC1 (b) and PC2 (c). TPS deformation mapped on *Hylopezus macularius* (A8409)



(b) PC1



(c) PC2

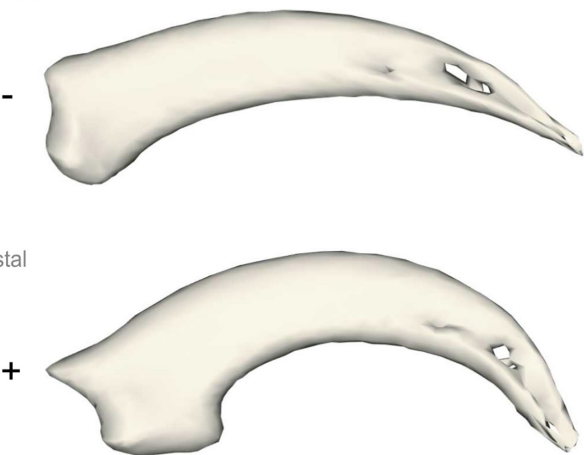


FIGURE 5 Geometric morphometric results for the ungual bone of the hallux. (a) PCA morphospace for the ungual bone of the hallux, a phylomorphospace is presented with the two main phylogenetic groups coloured (Furnariidae in blue, Dendrocolaptidae in red). Shape deformation at both Extrema along PC1 (b) and PC2 (c). TPS deformation mapped on *Hylopezus macularius* (A8409)

tests the significant interaction between phylogeny and morphological variation (Adams, 2014). The test returns a K value which evaluates whether the morphological similarities are higher than expected ($K > 1$, i.e. variation between clades) or lower than expected ($K < 1$, i.e. variation within clades) under a Brownian model of evolution between closely related species. To do so, we used the function “physignal” of the package Geomorph (Adams, 2014). All codes used to perform the analysis are available (SM8).

3 | RESULTS

We performed the geometric morphometrics analysis on all 15-foot bones (SM6 and SM7). Here, we present the results for the tarso-metatarsus, the proximal phalanges of all digits and the claw of digit I, which represent the bones with the higher percentage of cumulative explained variance for the two first axes (cumulative variance of the two first axis $> 55\%$).

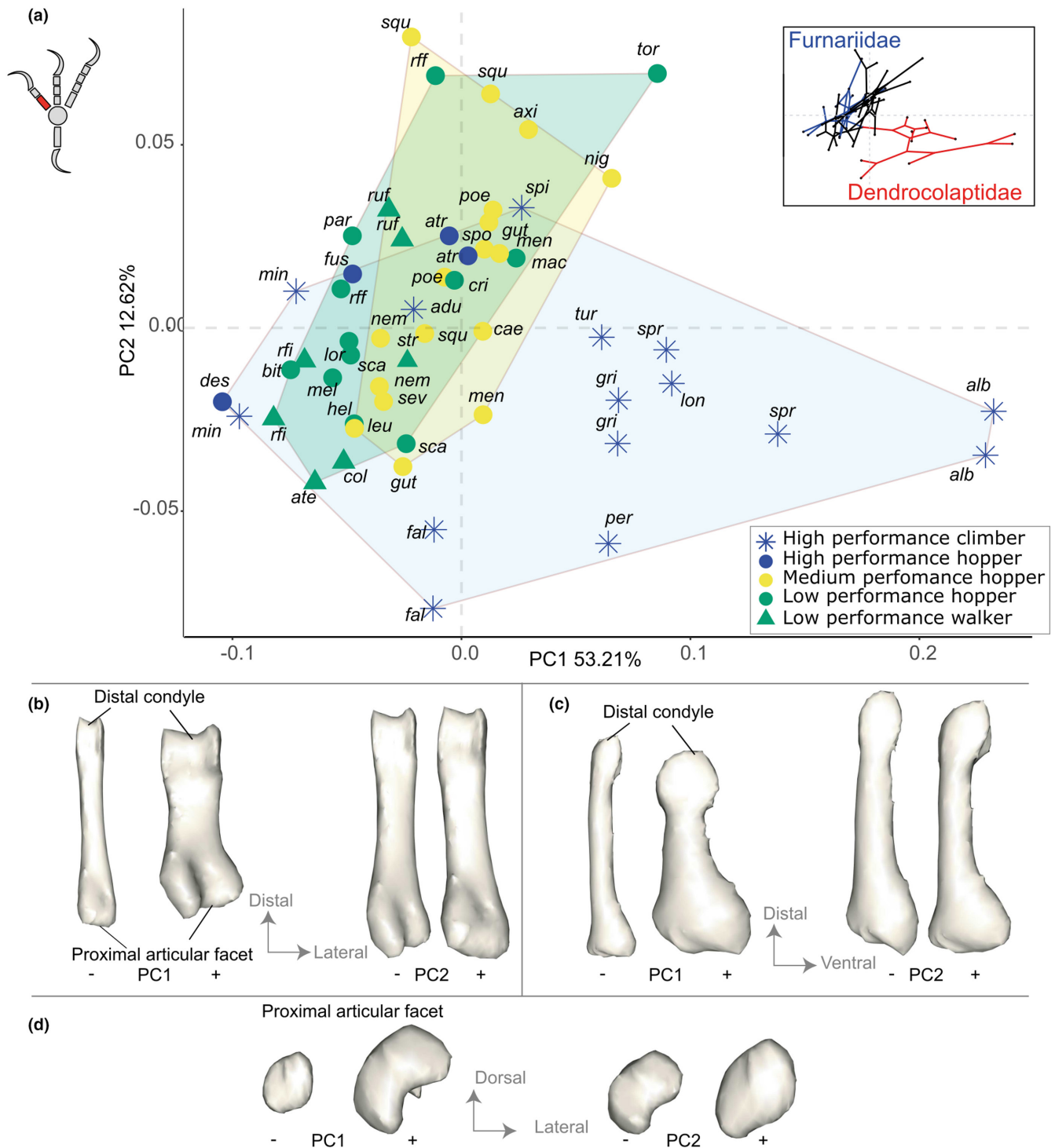


FIGURE 6 Geometric morphometric results for the first phalanx of the digit II. (a) PCA morphospace for the first phalanx of the digit II, a phylomorphospace is presented with the two main phylogenetic groups coloured (Furnariidae in blue, Dendrocolaptidae in red). Shape deformation at both Extrema along PC1 (left) and PC2 (right) in (b–d). TPS deformation mapped on *Hylopezus macularius* (A8409)

3.1 | Tarsometatarsus

The two first axes represent 51.63% and 12.29% of the variance, respectively, for a cumulative value of 63.92%. The low-performance group (in green Figure 3a) tends to occupy the negative scores of the PC1 whilst the high-performance group (in blue Figure 3a) occupies

the positive scores of the PC1. Both groups overlap with the medium-performance group (in yellow Figure 3a) around the mid-region of the PC1-PC2 morphospace. The medium-performance group is restricted to the centre upper part of the PC1-PC2 morphospace. *Xenopus minutus* (*min*), a climbing Furnariidae, is the most positive extreme of PC1, whilst *Myrmorchilus strigilatus* (*str*), a low-performance hopper, is the

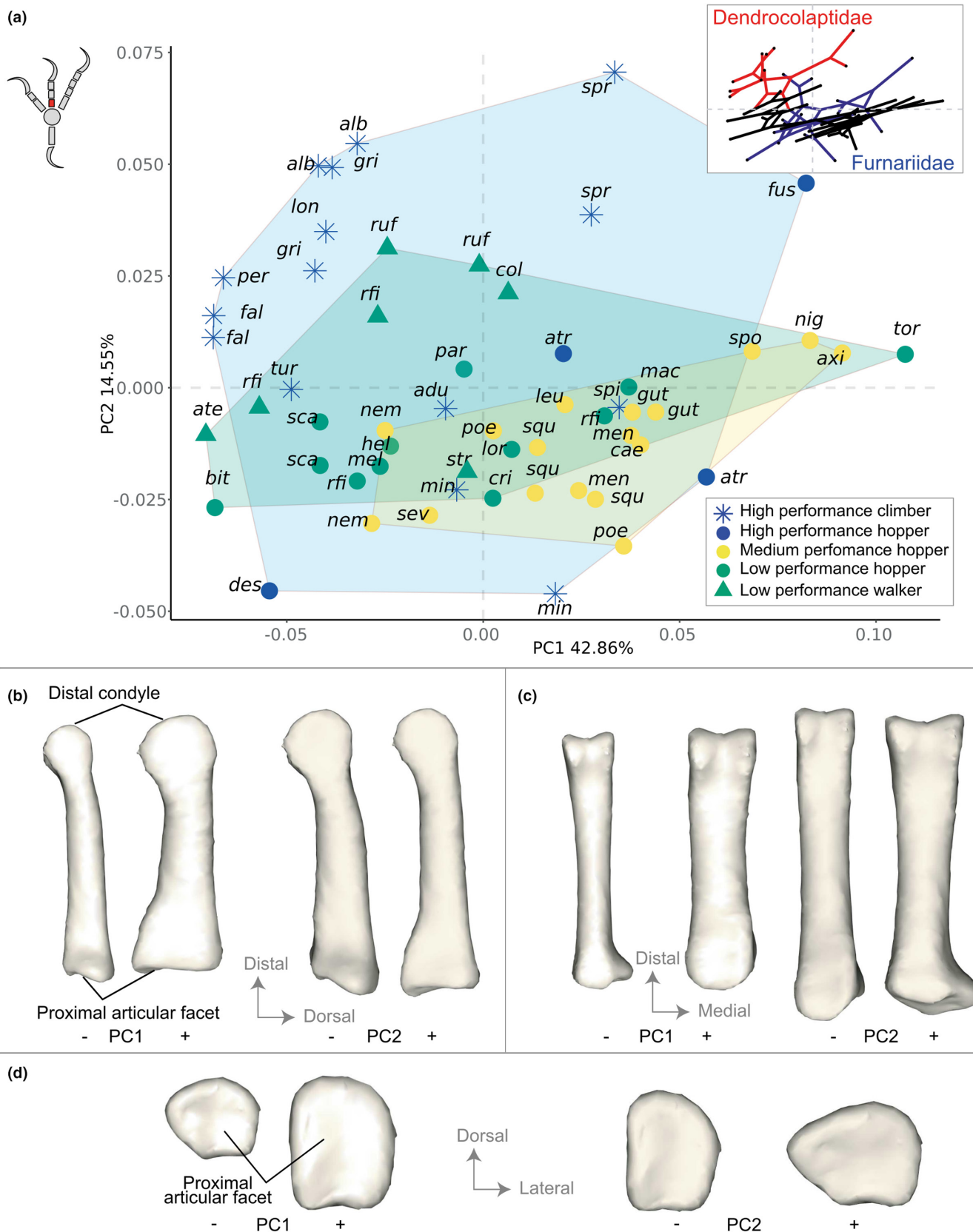


FIGURE 7 Geometric morphometric results for the first phalanx of the digit III. (a) PCA morphospace for the first phalanx of the digit III, a phylomorphospace is presented with the two main phylogenetic groups coloured (Furnariidae in blue, Dendrocolaptidae in red). Shape deformation at both Extrema along PC1 (left) and PC2 (right) in (b–d). TPS deformation mapped on *Hylopezus macularius* (A8409)

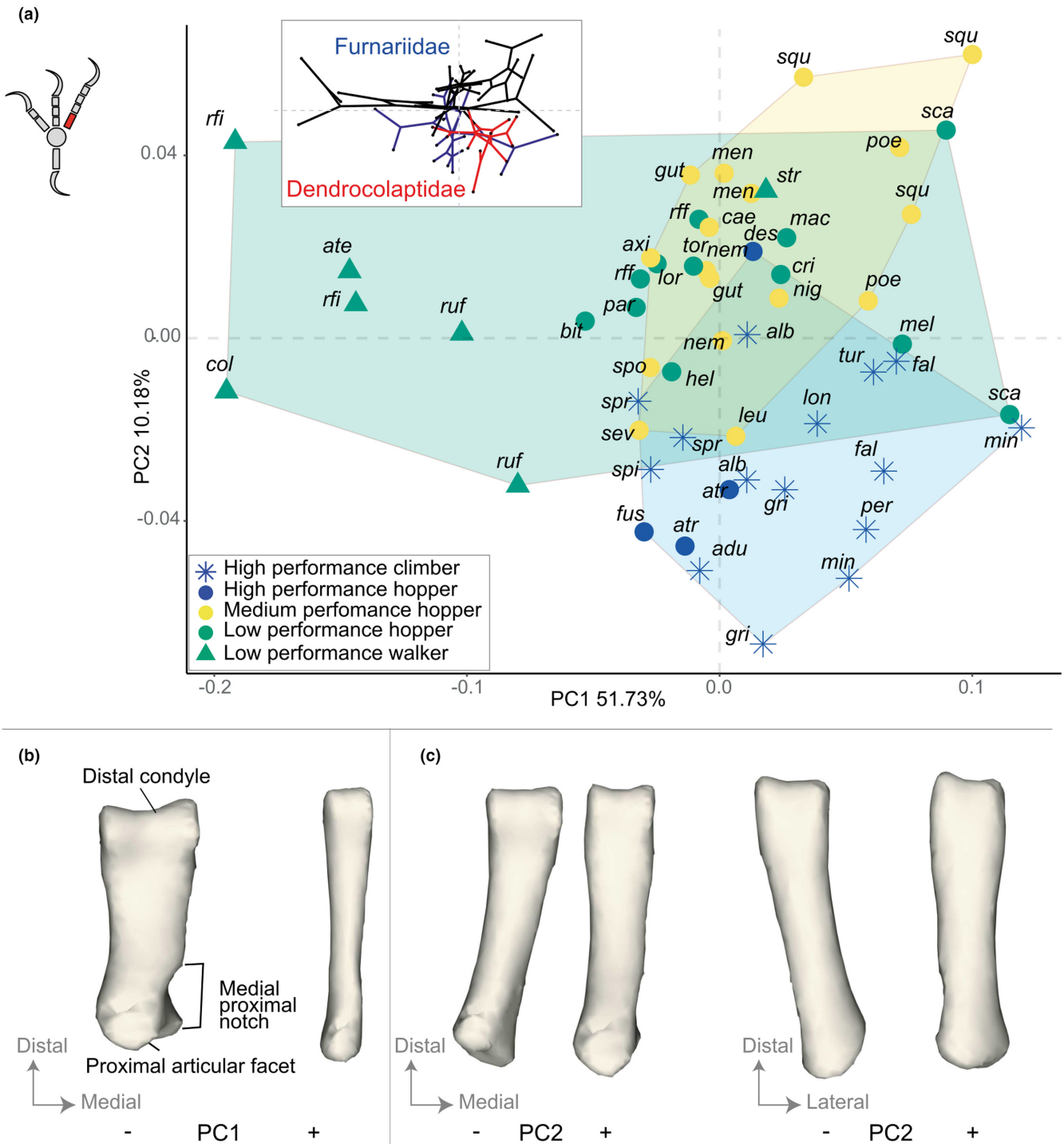


FIGURE 8 Geometric morphometric results for the first phalanx of the digit IV. (a) PCA morphospace for the first phalanx of the digit IV, a phylogenospaces is presented with the two main phylogenetic groups coloured (Furnariidae in blue, Dendrocolaptidae in red). Shape deformation at both Extrema along PC1 (b) and PC2 (c). TPS deformation mapped on *Hylopezus macularius* (A8409)

most negative extreme of PC1. On PC2, *Xiphocolaptes albicollis* (*alb*), a large and heavy climbing Dendrocolaptidae, is the negative extreme, whilst we found hopping birds, like *Euchrepomis spodioptila* (*spo*), *Dysithamnus mentalis* (*men*), *Drymophila squamata* (*squ*) or *Automolus leucophthalmus* (*leu*) in the most positive part of PC2.

The PC1 represents the distribution of gracile (negative side) against robust (positive side) conformations of the tarsometatarsus

(Figure 3b–f). At the positive part of PC1, the tarsometatarsus has relatively large structures in comparison to the shaft length and metatarsals are relatively large in all directions. Metatarsal I has an enlarged proximal part, inserted proximally into the shaft (Figure 3b, left) compared to the shape at the negative part of PC1. On the positive side of PC1, the tarsometatarsus has a large proximal end in all directions (Figure 3b,d,e). The ventral part of the lateral cotyle is

more prominent than the medial cotyle for the most robust shape (Figure 3e), whilst this is the opposite for the most gracile shape. These features, visible on the theoretical shape of positive PC1, can be defined as a more robust conformation.

The trochlea II and IV are large at the negative side of PC2 (Figure 3c, right). Trochleae II and IV extend strictly medially and laterally whilst trochlea I is more ventrally and proximally oriented (Figure 3c, right). Larger trochleae are paired with a larger lateral cotyle, extending laterally in the proximal end (Figure 3f, right). On the negative side of PC2, the ventral part of the lateral cotyle is high and prominent within the articulation, which contrasts with the other species having a lateral and medial cotyle at the same level (Figure 3d,e, right).

K's Bloomberg test at a multidimensional level shows a significant but weak interaction between the phylogeny and the global morphological variation (p -value <0.01 , $K_{\text{mult}} = 0.49$) accounting for all the PC scores. The same test at a unidimensional level also returned a significant and slightly stronger interaction for PC1 (p -value <0.01 , $K = 0.78$) and PC2 (p -value <0.01 , $K = 0.73$), but still lower than one, which indicates a similar morphological variation structured within several clades (~homoplastic) rather than between clades. Indeed, results from those tests indicate that closely related species resemble less to each other than more distantly related clades, according to expectations under a Brownian motion, which is represented here by the dispersion of the Furnariidae and Dendrocolaptidae family on the phylomorphospace (Figure 3a).

The result of the PGLS on every PC axis shows that there is a significant but low association between centroid sizes and the global morphology at a multidimensional level ($p < 0.01$, $R^2 = 0.13$), indicating evolutionary allometry in the tarsometatarsus. At a unidimensional level, we also find a low but significant size effect ($p < 0.01$, $R^2 = 0.31$), whereas there is a significant association between the centroid sizes and PC2 scores (p -value <0.05 , $R^2 = 0.12$).

3.2 | Phalanx I hallux

The two first axes represent 68.53% and 10.63% of the variance, respectively, for a cumulative value of 79.16% (Figure 4a).

High-performance species occupy a wider range than other species which are clustered in the positive region of the PC1, disregarding their locomotion mode and abilities. The shape of the phalanx of Dendrocolaptidae such as *Hylexetastes perrotii* (*per*) and *Xiphocolaptes albicollis* (*alb*) are represented in the most negative scores along PC1 whilst a hopping bird like *Willisornis poecilinotus* (*poe*) has the most positive values (Figure 4a). For the PC2, *Roraimia adusta* (*adu*) (a climber Furnariidae) represents the morphology at the most positive part whilst *Myrmotherula axillaris* (*axi*), an arboreal gleaner antbird, represents the morphology at the negative extreme (Figure 4a). The high-performance group has a wider range with climbing species restricted to the most negative part of the PC1, whilst the other species are restricted to the most positive part.

At the negative part of PC1, the phalanx I of the hallux is straighter and more robust than the shape at the positive part (Figure 4b). Robust phalanges have larger epiphyses extending dorsally. The proximal epiphysis is also flatter and more inclined than that of the gracile phalanges, which are thinner and rounded. Gracile phalanges are dorso-ventrally curved toward the dorsal side.

Locomotor modes are not sorted along PC2. Only climbing species are restricted to the positive side of the PC2, except for one specimen of *Glyphorhynchus spirurus* (*spr*) (one out of two), which extends the cluster into the negative side (Figure 4a). Every other taxon is spread out across the PC2, regardless of their locomotor modes and perching abilities (Figure 4a). The theoretical shape at the negative extreme of the PC2 has larger triangular epiphyses extending ventrally, whereas it is thinner and more rounded for the shape at the positive extreme (Figure 4c). Phalanges with thinner epiphyses are also straighter whilst larger phalanges are curvier toward the dorsal side (Figure 4c).

There is a significant but low interaction between phylogeny and the global morphological variation, which varies within different clades (p -value <0.01 , $K_{\text{mult}} = 0.67$). The variation along PC1 is significantly and strongly associated with the phylogeny and is structured between clades (p -value <0.01 , $K = 1.29$), whereas there is no significant association with the distribution along PC2 (p -value >0.05).

We highlight a significant but low allometry in the global morphological variation (i.e. including all PC axes; p -value <0.01 , $R^2 = 0.10$). At a unidimensional level (i.e. along each PC axis individually), we found a significant allometric effect along PC1 (p -value <0.01 , $R^2 = 0.21$). We also found a significant interaction along PC2 (p -value <0.01 , $R^2 = 0.16$).

3.3 | Ungual bone hallux

The two first axes represent 48.53% and 24.50% of the variance, respectively, for a cumulative value of 73.03% (Figure 5a).

The high-performance group occupies the negative part of the PC1 whilst the medium group occupies the positive part overlapping in the centre of the graph. Low performers spread out across PC1 and PC2. *Formicarius colma* (*col*), a walking terrestrial antthrush, and *Hylexetastes perrotii* (*per*), a woodcreeper, represent the extreme negative shapes. At the opposite, hooping understory birds like *Drymophila squamata* (*squ*) and *Dysithamnus mentalis* (*men*) are located in the most positive part. For the PC2, *Sittasomus griseicapillusi* (*gri*), a climbing Dendrocolaptidae, represents the most negative shape, whereas *Euchrepomis spodioptila* (*spo*), an agile Thamnophilidae, represents the most positive one.

The theoretical shape at the negative part of PC1 appears straighter than the one at the positive part because its tip region (i.e. the distal end of the unguis bone) is more dorsally oriented and its mid-shaft area is thinner (Figure 5b). Straighter bones in the negative part have a shorter flexor tubercle, oriented toward the proximal side, compared to curvier bones in the positive part, which have a

smaller flexor tubercle, oriented toward the ventral side. The proximal articular facet also extends more proximally for curvier shapes than in straighter ones.

Species are not sorted according to their locomotor or perching abilities along the PC2. The theoretical shape at the positive part of PC2 is curvier. The tip of the unguis bone is located more proximally and the flexor tubercle extends distally (Figure 5c) conversely to the shape at the negative part, which is straighter. The proximal articulation of the curvier shape is larger than the one of the straighter shapes (Figure 5c). The proximal articular facet extends ventrally, and the flexor tubercle extends proximally.

There is a significant but low phylogenetic signal on the global morphology (p -value <0.01 , $K_{\text{mult}} = 0.49$). For PC1 we also found a significant interaction that indicates a variation structured within clades (p -value <0.01 , $K = 0.78$) but not for PC2 (p -value >0.05).

There is no significant allometry, neither at a multidimensional (p -value >0.05) nor unidimensional level found using (p -value >0.05 for PC1 and PC2), meaning that size does not affect the unguis bone morphology.

3.4 | Phalanx I digit II

The two first axes represent 53.21% and 12.62% of the variance, respectively, for a cumulative value of 65.83% (Figure 6a). The high-performance group differs from the others by having a wider range associated with species occupying the positive part of the PC1. The other performance groups cluster in the negative part of the PC1. All groups overlap in the centre of the PC1–PC2 morphospace. For PC1, *Xiphocolaptes albicollis* (*alb*), a climbing woodcreeper, represents the most positive extreme whereas *Sylviorthorhynchus desmursi* (*des*), a foliage gleaner, is the most negative extreme. For PC2, *Campylorhamphus falcularius* (*fal*), a climbing Dendrocolaptidae, represents the extreme negative whilst hopping birds like *Drymophila squamata* (*squ*), *Phacellodomus rufifrons* (*rff*) and *Myrmornis torquata* (*tor*) are located in the most positive part.

High-performance groups spread across the PC1 with climbing species occupying the positive part of the PC1 (Figure 6a, in blue). The climbing species found in the positive part are Dendrocolaptidae (Figure 6a, polymorphospace). The theoretical shape at the positive part of PC1 is associated with a more robust phalanx (Figure 6b–d, left), whilst it is more gracile at the negative part. Robust phalanges have larger and more rounded distal condyles than gracile phalanges, which have more ovoid and thin distal condyles (Figure 6b,c, left). The proximal articular facet has a notable ventral notch (Figure 6b, left). The notch is deeper for the most robust shapes on the positive part than in the most gracile shapes on the negative part (Figure 6b, left).

Species are not sorted according to their locomotion abilities along the PC2 (Figure 6a). The shape at the positive part is associated with a proximal articular facet extending ventrally and distally (Figure 6b–d, right). In contrast, the distal part only extends ventrally conversely for the shape at the negative part (Figure 6b,c, right). PC1

represents the robusticity of the phalanx whilst PC2 represents the ventral expansions of the epiphyses (Figure 6b–d, right).

There is a significant but low interaction between the global morphology and the phylogeny (p -value <0.01 , $K = 0.53$). PC1 returns a greater significant interaction with the phylogeny (p -value <0.01 , $K = 0.88$). The low K value approaching one of PC1, indicating a variation structured within clades, still we observed that Dendrocolaptidae occupy the right part of the PC1 (Figure 6a, polymorphospace). There is no significant interaction with the phylogeny along PC2 (p -value >0.01).

There is no size effect at a multidimensional or unidimensional level (p -value >0.01).

3.5 | Phalanx I digit III

The two first axes represent 42.86% and 14.55% of the variance, respectively, for a cumulative value of 57.41%. All groups spread across the PCA disregarding the performance or the locomotion mode (Figure 7a) in consequence all groups overlap within the PCA. In the extreme positive part of PC1, we found *Myrmornis torquata* (*tor*), a terrestrial antbird, whilst on the opposite we found *Merulaxis ater* (*ate*) and *Melanopareia bitorquata* (*bit*), both terrestrial birds alongside climbing birds like *Campylorhamphus falcularius* (*fal*). For the second axis, *Xenops minutus* (*min*) and *Sylviorthorhynchus desmursii* (*des*) are at the most negative part, a climbing and an agile Furnariidae, respectively. At the positive part of PC2, we found *Glyphorhynchus spirurus* (*spr*) alongside others climbing birds from the Dendrocolaptidae.

Along the PC1, species spread across the PC1 disregarding their perching performance and locomotor mode (Figure 7a).

The shape in the most positive part of the PC1 is more robust than the shape in the negative part which is thinner in all directions, except for the proximal articular facet (Figure 7b–d, left). The proximal facet extends dorsally for the shape in the positive part, compared to the shape in the negative part, which has a lateral margin (Figure 7c).

Species are not sorted according to their locomotor mode nor to their perching performance along PC2 (Figure 7a).

The shape in the positive part of PC2 has a more robust distal condyle and a more developed lateral margin of the proximal articular facet than in the negative part (Figure 7b–d, right). The ventral part of the proximal articular facet is flat at the positive side of PC2 and inclined toward the distal side at the negative side of PC2 (Figure 7b–d, right).

There is a significant but low phylogenetic signal on the global morphological variation (p -value <0.01 , $K_{\text{mult}} = 0.41$). For PC1, there is also a significant interaction between phylogeny and morphological variation (p -value <0.01 , $K = 0.54$), as in PC2 (p -value <0.05 , $K = 0.46$). There is a significant but low allometry in the global morphological variation (p -value <0.05 , $R^2 = 0.04$). At a unidimensional level, we highlight allometry along PC1 (p -value <0.05 , $R^2 = 0.11$) but not PC2 (p -value >0.05).

3.6 | Phalanx I digit IV

The two first axes represent 51.73% and 10.18% of the variance, respectively, for a cumulative value of 61.91%.

The low-performance group occupies a wider range than the other groups across the PC1. *Chamaeza ruficauda* (*rfi*) and *Formicarius colma* (*col*) represent the extreme negative shape (Figure 8a, in green) at the opposite we found *Xenops minutus* (*min*), a climbing Furnariidae with *Sclerurus scansor* (*sca*), a terrestrial bird occasionally clinging on trunks. Species are not sorted according to their locomotion performances. Walking species tend to occupy the negative part of the PC1, except for *Myrmorchilus strigilatus* (*str*), a walking antbird.

The theoretical shape at the negative of PC1 is more robust with a proximal medial notch. The shapes at the positive part present a more gracile shape and lack the proximal medial notch (Figure 8b).

For PC2, *Sittasomus griseicapillus* (*gri*), a climbing Dendrocolaptidae, is the negative extreme, whilst *Drymophila squamata* (*squ*), an understory antbird represents the most positive shape (Figure 8a).

Specimens of the high-performance group occupy the most negative part of PC2, with species from Furnariidae and Dendrocolaptidae families. The rest overlaps with the other species from the other groups without distinction.

Amongst the PC2, species are not sorted according to their locomotor mode. At the most extreme negative shape, the phalanx is slightly larger, with a proximal part misaligned with its distal part, whilst the opposite is true at the positive part (Figure 8c).

There is a significant but low interaction between the global morphological variation and the phylogeny, which varies within different clades (p -value < 0.01 , $K_{\text{mult}} = 0.43$). The variation is significantly structured within different clades along PC1 (p -value < 0.01 , $K = 0.67$), and PC2 (p -value < 0.05 , $K = 0.40$). There is significant allometry at the global morphological variation (p -value < 0.05 , $R^2 = 0.04$) but not along PC1 and PC2 (p -value > 0.01).

3.7 | Two forms of syndactyly

3.7.1 | Dendrocolaptidae syndactyly

We observed a particular form of syndactyly between the first phalanx of digit II and III for the Dendrocolaptidae (Figure 9, Table 1). The lateral part of the first phalanx of digit II interlocks digit III. The proximal part of the first phalanx of digit III shows a medial expansion interlocking with the first phalanx of digit II. In the PCA of the first phalanx of digit III (Figure 7), we found that species spread out across the first axis, which represents the robusticity. On the second axis, Dendrocolaptidae and walking species tend to cluster in the positive part (Figure 7), such as *Furnarius rufus*, *Formicarius colma* and *Chamaeza ruficauda* and one acrobat, *Anabazenops fuscus*, which has phalanx with a lateral expansion of the proximal articular facet (Figure 7).

3.7.2 | Walking species syndactyly

We observed syndactyly between digits III and IV in the majority of walking species (Figure 9, Table 1). In the PCA of the first phalanx of digit IV (Figure 8), all walking species are clustered in the negative part of the PC1 except *Myrmorchilus strigilatus*. They are all associated with a theoretical shape robust paired with a medial notch whilst the other species have a thinner and gracile unnotched phalanx (Figure 8). *Furnarius rufus* is robust but does not have a medial notch, which is restricted to species found in the most negative shape.

3.8 | Other phalanges

Phalanges II digit III show a percentage of variance superior to 55% with 55.85 for the PC1 (SM2). High-performance climbers, corresponding to Dendrocolaptidae, tend to cluster on the positive part of PC2. Dendrocolaptidae has a more robust phalanx than other species except for *Dendrocolaptes turdina*, which overlap with low-performance groups (SM6c and SM7c)

The rest of the phalanges have a percentage of variance inferior to 50%. Although we will not describe the results further, they are available in SM6 and SM7

3.9 | Other claws

Our ungual bone analysis for the forward digits revealed a low percentage of variance. PC1 variance values are low and vary from 30% for digit IV to 37% for digit II. The ungual bone of the front digits are straighter and larger for low-performance birds, especially in walking species (SM6b, f and k, SM7b, f and k), whilst they are more curved and thinner in climbers (SM6b, f and k, SM7b, f and k).

4 | DISCUSSION

The morphological analysis of the foot of ovenbirds and woodcreepers (Furnariida) provides new insights into the morphological climbing adaptations within anisodactyl climbing birds.

4.1 | Tarsometatarsus

Our results showed that birds capable of high perching performances (i.e. birds commonly climbing on trees, hanging upside down or hanging down), tend to have a relatively robust tarsometatarsus (Figures 3–5a). *Xenops minutus*, a climbing Furnariidae, and *Xiphocolaptes albicollis*, a large and heavy climbing Dendrocolaptidae (Feduccia, 1973), both have robust tarsometatarsus (Figure 5a). We know that leg bones tend to be more robust in climbing birds (Carrascal et al., 1990; Norberg, 2008; Winkler & Bock, 1976), which

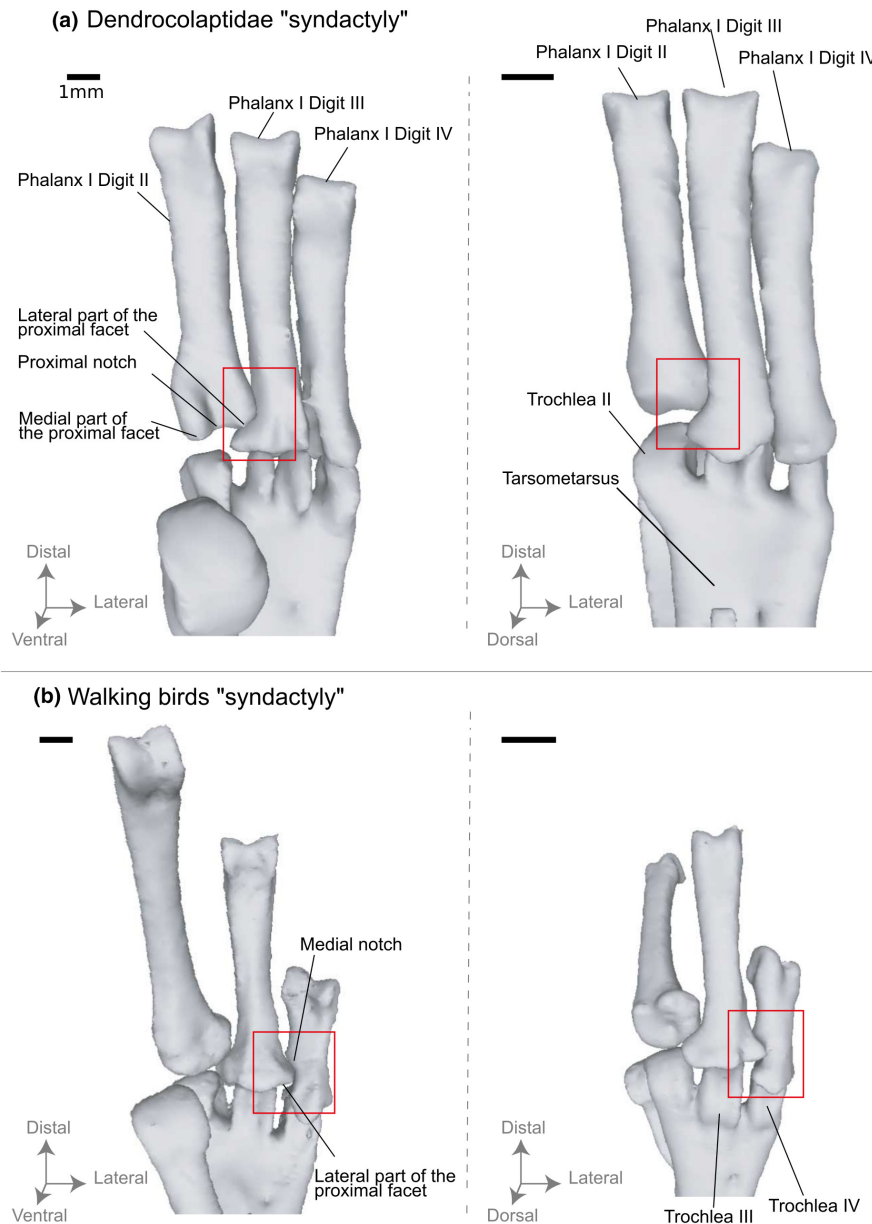


FIGURE 9 Figure showing the two forms of syndactyly. Syndactyly found in Dendrocolaptidae (a) with a ventral (left) and a dorsal (right) view of UFRJ1932 *Campylorhamphus falcularius*. Syndactyly found in walking Furnariidae (b) with a ventral (left) and a dorsal (right) view of UFRJ1932 *Campylorhamphus falcularius* (UFRJ1125 *Chamaeza ruficauda*). Scale bar = 1 mm

is thought to decrease the moment about the claw, subsequently reducing the force to keep the body close to the tree trunk (Zeffer et al., 2003). Here, we demonstrate that species known to cling to tree trunks (e.g. hopping birds with low-perching performance *Sclerurus scansor*) (Campos-Silva, 2013; Muscat et al., 2016; Van Els & Whitney, 2011) have a tarsometatarsus as robust as climbing birds, perching more often.

We also found a higher degree of separation between trochleae in high-perching performance species (Figure 3). This feature, associated with a wider spread of the toes may increase stability. It was previously observed in *Xiphorhynchus guttatus*, strong-billed wood-creeper (Feduccia, 1973). Qualitative observations (Feduccia, 1973) assessed that a wider spread between the toes was correlated to

better climbing performance. Although previous comparative studies between terrestrial and climbing birds suggest that, there is no clear correlation between toe spreading and climbing performances, our quantitative anatomical analysis showed that the degree of robusticity and trochleae spreading are both increasing along a gradient of locomotor performances (Figure 3a, Table 1). In this line, we observed that low- and medium-performance species (i.e. *Dendrocincla turdina*, a Dendrocolaptidae often perching Figure 3a; Skutch, 1996; Willis, 1972) are at an intermediate location on the robusticity and trochleae spreading gradients (i.e. between Furnariidae and high-performance Dendrocolaptidae). Even if categorising locomotor modes is challenging, our results show that accounting for performance level is crucial when interpreting the tarsometatarsus

morphology in ovenbirds and woodcreepers. Here, we propose that the degree of robusticity and trochleae spreading are reliable proxies for estimating acrobatic and climbing habits within the dataset.

4.2 | Syndactyly

4.2.1 | In climbers

The osteological study revealed a lateral expansion of the first phalanx of digit III, interlocking with a ventral notch in the first phalanx of digit II, amongst Dendrocolaptidae. Our results suggest that the robusticity of digit II is linked to the depth of its ventral notch: the more robust the phalanx, the deeper the notch (Figure 6).

So far, syndactyly, describing toes that share a common sheath of skin (Bock & Miller, 1959), was only described at the dermal level in Dendrocolaptidae (Feduccia, 1973). Here, even if we observed a fusion of the skin, we were able to separate the proximal phalanges of digits II and III during the segmentation process, assessing that the bones were not completely fused. However, the osteological features we described suggest a “functional osteological syndactyly” (Figure 9).

Previous studies found that dermal syndactyly is associated with a potential increase of friction forces (i.e. gripping forces) as it increases the surface between the foot and the substrate (Höfling & Abourachid, 2021), hereby confirming the potential adaptation in high-performance species. The mechanical advantage of syndactyly at an osteological level needs to be further explained, through biomechanical analyses. We can still hypothesise that the interlocking of the two toes could work in tandem with external syndactyly as we found that the length of the dermal syndactyly between digit II and III is more important for Dendrocolaptidae as it extended to the entire first phalanx of the digit II (SM3c). We could wonder how could the dermal syndactyly and the bone morphology improve the climbing performance need to be tested in future work, ideally by comparing the morphology and performance of Dendrocolaptidae with other climbing birds like Picidae (Woodpeckers) and Certhiidae (nuthatches and allies).

When present, syndactyly is located on forward toes in birds using their tail to climb (woodpeckers and Dendrocolaptidae) (Scharnke, 1930). Interestingly, we did not observe any functional osteological syndactyly amongst Furnariidae, which are not using their tail but rely exclusively on the force of their feet to climb. A punctual observation of Furnariidae (Skutch, 1996) reported that these birds climb like nuthatches (<https://macaulaylibrary.org/asset/262249381>; <https://macaulaylibrary.org/asset/200800521>), with their body oriented horizontally and with one leg above the centre of mass, whilst the other leg remains below (Cartmill, 1985). However, unlike nuthatches, climbing Furnariidae are unable to descend tree trunks headfirst. This suggests a specific way of climbing, which could explain the leg adaptations, exclusive to Furnariidae. Indeed, the hallux and digit II of Furnariidae are more elongated and slender than that of Dendrocolaptidae (Figures 4 and 6).

4.2.2 | In walkers

Our detailed anatomical analysis also revealed a different form of syndactyly amongst walking species (e.g. in *Chamaeza ruficauda*, *Formicarius colma*, *Merulaxis ater*). The first phalanx of digits III and IV are interlocked through a medial notch on digit IV, connected to the proximal part of the first phalanx of digit III. In *Furnarius rufus*, a walking Furnariidae, the notch is superficial on the first phalanx of digit IV, but the phalanx is still robust and is closely in contact with the other phalanx. *Myrmorchilus strigilatus*, a walking Thamnophilidae, is the only walking species of our sample without syndactyly. It is still unknown how the syndactyly between digits III and IV could be beneficial for walking from a functional point of view. Further biomechanical studies should be conducted to understand its role better.

4.3 | Hallux

We know that Dendrocolaptidae use their modified tail feathers for support when climbing (Claramunt et al., 2012), unlike Furnariidae (Tubaro et al., 2002). In our data, Dendrocolaptidae differ from other climbing species by having robust first phalanges for the hallux and digit II. This is especially shown by the morphological variation of the hallux being influenced by the taxonomic differentiation, as demonstrated by its significant and strong phylogenetic signal (Figure 4a,k = 1, 29 p -value <0.05). Because toes pointing forward (i.e. digits II, III and IV in anisodactyl birds) provide a stronger grip on the tree trunk and pull out the body when climbing up (Bock & Miller, 1959), we could hypothesise that toes pointing forward are more likely to evolve climbing adaptations than toes pointing downward (i.e. hallux in anisodactyl birds). However, our results revealed a robust first phalanx of the hallux amongst Dendrocolaptidae (Figures 4b and 5b), which is a trait commonly associated with climbing birds (Abourachid et al., 2017). It suggests that the hallux could contribute more than initially thought in the climbing efficiency. Maybe Dendrocolaptidae could orient their tarsometatarsus laterally during climbing, which would reorient the toes more laterally and the hallux more medially to provide a greater grasp onto the trunk. This toe configuration would be particularly useful when climbing on horizontal or inclined trunks. It was punctually observed in *Glyphorynchus spirurus* (e.g. <https://macaulaylibrary.org/asset/201958771>). Other climbing birds use this mechanism as well, like woodpeckers, amongst which downward toes (i.e. hallux & digit IV in zygodactyl birds) are reoriented forward or laterally during climbing (Bock & Miller, 1959).

4.4 | Claws

Our ungual bone analysis showed that the front digits are straighter and larger for low-performance birds, especially in walking species (SM6b, e and i, SM7b, e and i), whilst they are more curved and thinner in climbers (SM6b, e and i, SM7b, e and i). We know that

front digits tend to grip the tree trunk to provide support at rest and pull out the body when climbing up. Thus, a curved claw seems to be adapted to this function (Bock & Miller, 1959). Our data show that the hallux unguis bones are not following the same trend as the front digits: they are straighter for climbers and more curved for medium-performance birds and acrobats such as *Hypodaleus guttatus*, *Philydor atricapillus* and *Anabazenops fuscus* (Figure 5a). Comparative dissections (Raikow, 1993) revealed stronger *M. flexor hallucis longus* with heavy ossification in *Hylexetastes perrotii*, a climbing Dendrocolaptidae, compared to *Lochmias nematura*, a non-climbing Furnariidae (Figure 5a). Since this muscle is attached to the flexor tubercle (Figure 5b) (Backus et al., 2015), it is involved in the flexion of the hallux claw (Raikow, 1993). Our osteological analysis of the hallux shows that the flexor tubercle is oriented more proximally in Dendrocolaptidae. It could be associated with an increase of the *M. flexor hallucis longus* lever arm and thus of the force produced by this muscle. As the first phalanx of the hallux, articulating with the claw, is more robust in Dendrocolaptidae, which is a characteristic of climbing species (Abourachid et al., 2017; Zeffler et al., 2003), our result suggests that the hallux could be used during climbing, even if the claw is straight. Future studies should consider covariation between the foot bones (Kavanagh et al., 2013), especially between phalangeal bones, which are articulating together and closely in contact because of the syndactyly. Considering our results, we expect a covariation between the first phalanx of the hallux and digit II, and of the claw, associated with their potential role during climbing Dendrocolaptidae.

We ignore if the *M. flexor hallucis longus* shows a similar condition in climbing Furnariidae due to a lack of myological studies in climbing species of this group. Quantitative dissections of the different muscles of the ovenbirds and woodcreepers, associated with claw flexion/extension analysis, would provide valuable information on their potential role in climbing. Similarly, we ignore how a straight claw could provide support for climbing. A biomechanical analysis of claw attachment during climbing or acrobatic manoeuvre could help to clarify the morphological adaptation of the unguis bones.

5 | CONCLUSIONS

By focusing on the foot, we were able to find subtle morphological adaptations associated with specific ways of climbing (e.g. tail-assisted climbing or not), using state-of-the-art 3D GMM. In general, climbing species tend to have a more robust tarsometatarsus, with highly spread trochlea. The presence of a notch in the first phalanx of digit IV, interlocking with the first phalanx of digit III, associated with dermal syndactyly can be interpreted as functional osteological syndactyly, certainly improving the climbing ability of these birds. Finally, climbing species are more likely to have strongly curved claws on their forward digits (digits II, III and IV).

In addition to the 15 bones studied here, other long leg bones, like the femur or the tibiotarsus, should present morphological

adaptations and are worthy of interest. Our work, revealing adaptations to high locomotor performance in Furnariidae lays the foundation for exploring the anatomy of two other groups of climbing birds: Picidae (Woodpeckers) and Certhioidae (nuthatches and allies).

AUTHOR CONTRIBUTIONS

Killian Leblanc: analysis, investigation, figure, table, visualisation—main analysis and writing—original draft, review and editing. Romain Pintore: formal analysis, investigation, methodology, supervision, visualisation and writing—original draft, review and editing. Ana Galvão: conceptualisation, sample collection, data curation, investigation and writing—review and editing. Ezekiel Heitz: investigation, software and validation. Pauline Provini: conceptualisation, data curation investigation, supervision, funding acquisition, project administration, resources and writing—review and editing.

ACKNOWLEDGMENTS

The authors would like to thank the Programa Nacional de Pós-Doutorado (PNPD) da Coordenação de Aperfeiçoamento Pessoal de Nível Superior (CAPES, Brazil). Thanks to Enio Mattos and Phillip Lenkaitis from the Departamento de Zoologia of the Instituto de Biociências, Universidade de São Paulo, Brazil for the assistance with the CT scans and to Luiz Pedreira Gonzaga (Universidade Federal do Rio de Janeiro, Rio de Janeiro, Brazil) and Alexandre Aleixo (Museu Paraense Emílio Goeldi, Pará, Brazil) for lending key specimens used in this work.

We thank MorphoSource (www.morphosource.org) for making the CT scan available. Creation of datasets accessed on MorphoSource was made possible by the following funders and grant numbers: Roger Benson provided access to these data, originally appearing in Lowi-Merri et al. (2021) BMC Biology “The relationship between sternum variation and mode of locomotion in birds”, the collection of which was funded by the European Research Council (ERC) starting grant TEMPO (ERC-2015-STG-677774) to Roger Benson. The files were downloaded from www.MorphoSource.org, Duke University, Migrated MorphoSource 1 Media Citation Instructions: Field Museum of Natural History provided access to these data, the collection of which was funded by oVert TCN. The files were downloaded from www.MorphoSource.org, Duke University, Migrated MorphoSource 1 Media Citation Instructions: University of Kansas Natural History Museum provided access to these data, the collection of which was funded by oVert TCN. The files were downloaded from www.MorphoSource.org, Duke University.

We would like to thank the Macaulay Library at the Cornell Lab of Ornithology and their community as they provided us with crucial information about the birds present in this study. We used the following recordings from the Macaulay Library at the Cornell Lab of Ornithology: ML66570301 and ML33078331. We are grateful to Alexandra Houssaye and the “Gravibone team” for hosting Killian Leblanc during the data analysis. Thanks to the Bettencourt Schueller Foundation long-term partnership, this work was partly supported by the CRI Research Fellowship to Pauline Provini.

FUNDING INFORMATION

Programa Nacional de Pós-Doutorado (PNPD) da Coordenação de Aperfeiçoamento Pessoal de Nível Superior (CAPES, Brasil). The Bettencourt Schueller Foundation long-term partnership, this work was partly supported by the CRI Research Fellowship to Pauline Provini.

CONFLICT OF INTEREST

All authors present in this have no conflict of interest to declare that could bias this study.

DATA AVAILABILITY STATEMENT

The data underlying this article are publicly available on Github at the following URL: <https://github.com/BirdsongTeam/Supplementary-Material-Leblanc-Pintore-et-al>.

ORCID

Romain Pintore  <https://orcid.org/0000-0003-2438-614X>

Ana Galvão  <https://orcid.org/0000-0002-6449-7293>

Pauline Provini  <https://orcid.org/0000-0002-9374-1291>

REFERENCES

- Abourachid, A., Fabre, A.-C., Cornette, R. & Höfling, E. (2017) Foot shape in arboreal birds: two morphological patterns for the same pincer-like tool. *Journal of Anatomy*, 231, 1–11.
- Adams, D., Collyer, M. & Kaliontzopoulou, A. (2022) geomorph: Geometric Morphometric Analyses of 2D/3D Landmark Data. Available from: <https://CRAN.R-project.org/package=geomorph> [Accessed 17th May 2022].
- Adams, D.C. (2014) A method for assessing phylogenetic least squares models for shape and other high-dimensional multivariate data: PGLS for high-dimensional data. *Evolution*, 68, 2675–2688. Available from: <https://doi.org/10.1111/evo.12463>
- Backus, S.B., Sustaita, D., Odhner, L.U. & Dollar, A.M. (2015) Mechanical analysis of avian feet: multiarticular muscles in grasping and perching. *Royal Society Open Science*, 2, 140350. Available from: <https://doi.org/10.1098/rsos.140350>
- Blomberg, S.P., Garland, T. & Ives, A.R. (2003) Testing for phylogenetic signal in comparative data: behavioral traits are more labile. *Evolution*, 57, 717–745. Available from: <https://doi.org/10.1111/j.0014-3820.2003.tb00285.x>
- Bock, W.J. (1999) Functional and evolutionary morphology of woodpeckers. *Ostrich*, 70, 23–31. Available from: <https://doi.org/10.1080/00306525.1999.9639746>
- Bock, W.J. & Miller, W.D. (1959) The scansorial foot of the woodpeckers, with comments on the evolution of perching and climbing feet in birds. *American Museum novitates*; no. 1931. Available from: <http://hdl.handle.net/2246/5316>
- Botton-Divet, L., Houssaye, A., Herrel, A., Fabre, A.C. & Cornette, R. (2015) Tools for quantitative form description; an evaluation of different software packages for semi-landmark analysis. *PeerJ*, 3, e1417. Available from: <https://doi.org/10.7717/peerj.1417>
- Campos-Silva, J. (2013) Roost of Leaf-tossers (genus *Sclerurus*) in the Brazilian Amazon: hints of the low density in fragmented environments. *Revista Brasileira de Ornitologia*, 21, 129–132.
- Carrascal, L.M., Moreno, E. & Tellería, J.L. (1990) Ecomorphological relationships in a group of insectivorous birds of temperate forests in winter. *Ecography*, 13, 105–111. Available from: <https://doi.org/10.1111/j.1600-0587.1990.tb00595.x>
- Cartmill, M. (1985) Chapter 5. Climbing. In: Hildebrand, M., Bramble, D.M., Liem, K.F., Liem, K.F. & Wake, D.B. (Eds.) *Functional vertebrate morphology*. Harvard University Press, pp. 73–88. Available from: <https://doi.org/10.4159/harvard.9780674184404.c5>
- Claramunt, S., Derryberry, E.P., Brumfield, R.T. & Remsen, J.V., Jr. (2012) Ecological opportunity and diversification in a continental radiation of birds: climbing adaptations and cladogenesis in the Furnariidae. *The American Naturalist*, 179, 649–666.
- Cornette, R., Baylac, M., Souter, T. & Herrel, A. (2013) Does shape co-variation between the skull and the mandible have functional consequences? A 3D approach for a 3D problem. *Journal of Anatomy*, 223, 329–336. Available from: <https://doi.org/10.1111/joa.12086>
- Feduccia, A. (1973) Evolutionary trends in the Neotropical ovenbirds and woodhewers. *Ornithological Monographs*, 13, i–69.
- Fraga, R.M. (1980) The breeding of rufous Horneros (*Furnarius rufus*). *The Condor*, 82, 58–68. Available from: <https://doi.org/10.2307/1366785>
- Gunz, P. & Mitteroecker, P. (2013) Semilandmarks: a method for quantifying curves and surfaces. *Hystrix, the Italian Journal of Mammalogy*, 24. Available from: <https://doi.org/10.4404/hystrix-24.1-6292>
- Gunz, P., Mitteroecker, P. & Bookstein, F.L. (2005) Semilandmarks in three dimensions. In: Slice, D.E. (Ed.) *Modern morphometrics in physical anthropology*. New York: Kluwer Academic Publishers-Plenum Publishers, pp. 73–98. Available from: https://doi.org/10.1007/0-387-27614-9_3
- Hedrick, B.P., Cordero, S.A., Zanno, L.E., Noto, C. & Dodson, P. (2019) Quantifying shape and ecology in avian pedal claws: the relationship between the bony core and keratinous sheath. *Ecology and Evolution*, 9, 11545–11556. Available from: <https://doi.org/10.1002/ece3.5507>
- Höfling, E. & Abourachid, A. (2021) The skin of birds' feet: morphological adaptations of the plantar surface. *Journal of Morphology*, 282, 88–97. Available from: <https://doi.org/10.1002/jmor.21284>
- Irestedt, M., Fjeldsaa, J., Johansson, U.S. & Ericson, P.G. (2002) Systematic relationships and biogeography of the tracheophone suboscines (Aves: Passeriformes). *Molecular Phylogenetics and Evolution*, 23, 499–512.
- Kavanagh, K.D., Shoval, O., Winslow, B.B., Alon, U., Leary, B.P., Kan, A. et al. (2013) Developmental bias in the evolution of phalanges. *Proceedings of the National Academy of Sciences of the United States of America*, 110, 18190–18195. Available from: <https://doi.org/10.1073/pnas.1315213110>
- Klingenberg, C.P. (2016) Size, shape, and form: concepts of allometry in geometric morphometrics. *Development Genes and Evolution*, 226, 113–137. Available from: <https://doi.org/10.1007/s00427-016-0539-2>
- Krabbe, N.K. & Schulenberg, T.S. (2003) Family Formicariidae (ground antbirds). In: del Hoyo, J., Elliott, A., Sargatal, J. & Christie, D.A. (Eds.) *Handbook of the birds of the world*. Barcelona, Spain: Lynx Edicions, pp. 682–731.
- Lowi-Merri, T.M., Benson, R.B.J., Claramunt, S. & Evans, D.C. (2021) The relationship between sternum variation and mode of locomotion in birds. *BMC Biology*, 19(1), 1–23.
- Maddison, W. & Maddison, D. (2007) Mesquite 2: a modular system for evolutionary analysis. *Evolution*, 62, 1103–1118.
- Moyle, R.G., Chesser, R.T., Brumfield, R.T., Tello, J.G., Marchese, D.J. & Cracraft, J. (2009) Phylogeny and phylogenetic classification of the antbirds, ovenbirds, woodcreepers, and allies (Aves: Passeriformes: infraorder Furnariidae). *Cladistics*, 25, 386–405. Available from: <https://doi.org/10.1111/j.1096-0031.2009.00259.x>
- Muscat, E., Rotenberg, E.L. & Tanaka, R.M. (2016) *Sclerurus macconelli* may use roosting sites with high fidelity. *Atualidades Ornitológicas*, 192, 27.
- Norberg, R.Å. (2008) Why foraging birds in trees should climb and hop upwards rather than downwards. *Ibis*, 123, 281–288. Available from: <https://doi.org/10.1111/j.1474-919X.1981.tb04030.x>

- Ohlson, J.I., Irestedt, M., Ericson, P.G. & Fjelds , J.O.N. (2013) Phylogeny and classification of the New World suboscines (Aves, Passeriformes). *Zootaxa*, 3613, 1–35.
- Pacheco, J.F., Whitney Bret, M. & Gonzaga, L.P. (1996) A new genus and species of furnariid (Aves: Furnariidae) from the cocoa-growing region of southeastern Bahia, Brazil. *The Wilson Bulletin*, 108, 397–433.
- Parrini, R., Pacheco, J.F. & Mallet-Rodrigues, F. (2010) Comportamento de forrageamento de Philydor atricapillus (Passeriformes: Furnariidae) na Floresta Atl ntica do Estado do Rio de Janeiro, regi o Sudeste do Brasil. *Atualidades Ornitol gicas On-line*, 153, 55–61.
- Provini, P. & H fing, E. (2020) To hop or not to hop? The answer is in the bird trees. *Systematic Biology*, 69, 962–972. Available from: <https://doi.org/10.1093/sysbio/syaa015>
- Raikow, R.J. (1993) Structure and variation in the hindlimb musculature of the woodcreepers (Aves: Passeriformes: Dendrocolaptinae). *Zoological Journal of the Linnean Society*, 107, 353–399. Available from: <https://doi.org/10.1111/j.1096-3642.1993.tb00291.x>
- Raikow, R.J. (1994) Climbing adaptations in the hindlimb musculature of the woodcreepers (Dendrocolaptinae). *Condor*, 96, 1103–1106.
- Rohlf, F.J. (1990) Morphometrics. *Annual Review of Ecology and Systematics*, 21, 299–316. Available from: <https://doi.org/10.1146/annurev.es.21.110190.001503>
- Scharnke, H. (1930) Physiologisch-anatomische Studien am Fu  der Spechte. *Journal f r Ornithologie*, 78, 308–327. Available from: <https://doi.org/10.1007/BF01953326>
- Schlager, S. (2017) Morpho and Rvcg – shape analysis in R. In: Zheng, G., Li, S. & Szekely, G. (Eds.) *Statistical shape and deformation analysis*. Elsevier, pp. 217–256. Available from: <https://doi.org/10.1016/B978-0-12-810493-4.00011-0>
- Sick, H., Haffer, J., Alvarenga, H.F., Pacheco, J.F. & Barruel P. (1997) *Ornitologia brasileira Ed. rev. e ampliada por Jos  Fernando Pacheco*. Rio de Janeiro: Editora Nova Fronteira.
- Skutch, A.F. (1996) *Antbirds and ovenbirds: their lives and homes*. Austin, TX: University of Texas Press.
- Spring, L.W. (1965) Climbing and pecking adaptations in some north American woodpeckers. *The Condor*, 67, 457–488. Available from: <https://doi.org/10.2307/1365612>
- Team RC. (2021) *R: A language and environment for statistical computing (Version 4.0. 5) [Computer software]*. Vienna: R Foundation for Statistical Computing.
- Team RC, Team MRC, Suggests M & Matrix, S. (2018) Package stats. The R Stats Package.
- Tubaro, P.L., Lijtmaer, D.A., Palacios, M.G. & Kopuchian, C. (2002) Adaptive modification of tail structure in relation to body mass and buckling in woodcreepers. *The Condor*, 104, 281–296.
- Van Els, P. & Whitney, B.M. (2011) Arboreal roosting as a possible explanation for tail stiffness in the genus *Sclerurus*. *Ornitologia Neotropical*, 22, 477–479.
- Wiley, D.F., Amenta, N., Alcantara, D.A., Ghosh, D., Kil, Y.J., Delson, E. et al. (2005) Evolutionary morphing. Available: <https://escholarship.org/uc/item/4k5991zk>. Accessed 17 May 2022.
- Willis, E.O. (1972) The behavior of plain-brown Woodcreepers, *Dendrocincla fuliginosa*. *Wilson Bulletin*, 84, 377–420.
- Winkler, H. & Bock, W.J. (1976) Analyse der Kr fteverh ltnisse bei Kletterv geln. *J f r Ornithol*, 117, 397–418. Available from: <https://doi.org/10.1007/BF01647169>
- Zeffer, A., Johansson, L.C. & Marmebro, A. (2003) Functional correlation between habitat use and leg morphology in birds (Aves). *Biological Journal of the Linnean Society*, 79, 461–484.

SUPPORTING INFORMATION

Additional supporting information can be found online in the Supporting Information section at the end of this article.

How to cite this article: Leblanc, K., Pintore, R., Galv o, A., Heitz, E. & Provini, P. (2023) Foot adaptation to climbing in ovenbirds and woodcreepers (Furnariida). *Journal of Anatomy*, 242, 607–626. Available from: <https://doi.org/10.1111/joa.13805>